The *Saccharomyces cerevisiae* Actin Patch Protein App1p Is a Phosphatidate Phosphatase Enzyme[*][♦]

Minjung Chae, Gil-Soo Han, and George M. Carman[1]

From the Department of Food Science, Rutgers Center for Lipid Research, and New Jersey Institute for Food, Nutrition, and Health, Rutgers University, New Brunswick, New Jersey 08901

Background: Phosphatidate phosphatase (PAP) plays diverse roles in lipid metabolism and cell signaling.
Results: A novel yeast PAP is identified as the actin patch protein encoded by *APP1*.
Conclusion: *APP1* and other known genes (*PAH1*, *DPP1*, *LPP1*) are responsible for all detectable PAP activity in yeast.
Significance: Identification of App1p as a PAP enzyme will facilitate the understanding of its cellular function.

Phosphatidate phosphatase (PAP) catalyzes the dephosphorylation of phosphatidate to yield diacylglycerol. In the yeast *Saccharomyces cerevisiae*, PAP is encoded by *PAH1*, *DPP1*, and *LPP1*. The presence of PAP activity in the *pah1Δ dpp1Δ lpp1Δ* triple mutant indicated another gene(s) encoding the enzyme. We purified PAP from the *pah1Δ dpp1Δ lpp1Δ* triple mutant by salt extraction of mitochondria followed by chromatography with DE52, Affi-Gel Blue, phenyl-Sepharose, MonoQ, and Superdex 200. Liquid chromatography/tandem mass spectrometry analysis of a PAP-enriched sample revealed multiple putative phosphatases. By analysis of PAP activity in mutants lacking each of the proteins, we found that *APP1*, a gene whose molecular function has been unknown, confers ∼30% PAP activity of wild type cells. The overexpression of *APP1* in the *pah1Δ dpp1Δ lpp1Δ* mutant exhibited a 10-fold increase in PAP activity. The PAP activity shown by App1p heterologously expressed in *Escherichia coli* confirmed that *APP1* is the structural gene for the enzyme. Introduction of the *app1Δ* mutation into the *pah1Δ dpp1Δ lpp1Δ* triple mutant resulted in a complete loss of PAP activity, indicating that distinct PAP enzymes in *S. cerevisiae* are encoded by *APP1*, *PAH1*, *DPP1*, and *LPP1*. Lipid analysis of cells lacking the PAP genes, singly or in combination, showed that Pah1p is the only PAP involved in the synthesis of triacylglycerol as well as in the regulation of phospholipid synthesis. App1p, which shows interactions with endocytic proteins, may play a role in vesicular trafficking through its PAP activity.

PAP[2] catalyzes the dephosphorylation of PA to produce DAG and P_i (1). The product DAG is utilized for the synthesis of the neutral storage lipid TAG and for the synthesis of the phospholipids phosphatidylcholine and phosphatidylethanolamine via the Kennedy pathway (1–6). The substrate PA is utilized for the synthesis of phospholipids (*e.g.* phosphatidylinositol, phos-

phatidylglycerol, and cardiolipin) via the liponucleotide intermediate CDP-DAG (7–9). In addition to serving as intermediates in lipid synthesis, PA and DAG are involved in lipid signaling. For example, PA plays a role in cell growth activation, membrane proliferation, the transcription of lipid synthesis genes, secretion, and vesicular transport, whereas DAG activates protein kinase C (10–20). Thus, by the nature of its reaction, PAP activity may regulate the proportional synthesis of phospholipids and TAG, the pathways by which phospholipids are synthesized, and control the abundance of important signaling lipids. Indeed, biochemical and genetic studies using yeast and mammalian experimental systems have shown that PAP is an important regulator of lipid homeostasis and cell physiology (21–25).

Our laboratory has utilized the yeast *Saccharomyces cerevisiae* as a model eukaryote to study the enzymology and physiological roles of PAP enzymes (22, 26). In *S. cerevisiae*, PAP is known to be encoded by three genes, namely *PAH1* (27), *DPP1* (28), and *LPP1* (29). Pah1p PAP is a Mg^{2+}-dependent enzyme whose reaction is based on the DXDX(T/V) catalytic motif within the haloacid dehalogenase-like domain of the enzyme (27, 30). In contrast, the PAP activities of Dpp1p (28) and Lpp1p (29) do not have a divalent cation requirement, and their reactions are based on a three-domain lipid phosphatase motif composed of the consensus sequences KX_6RP, PSGH, and SRX_5HX_3D (31, 32). The Pah1p enzyme is specific for PA (27), whereas the Dpp1p and Lpp1p enzymes utilize PA and other lipid phosphate molecules (*e.g.* DAG pyrophosphate and lysoPA) as substrates (28, 29, 33–36). The PAP activities in yeast also differ with respect to their cellular locations and modes of regulation. Pah1p is found in the cytosol as a phosphoprotein that is a consequence of multiple phosphorylations (37–40). For catalysis, the phosphorylated enzyme translocates to the nuclear/endoplasmic reticulum membrane through its dephosphorylation (38, 41–43). Dpp1p (28, 44, 45) and Lpp1p (29, 46) are integral membrane enzymes with six transmembrane-spanning regions that are localized to the vacuole and Golgi compartments, respectively, of the cell.

Pah1p PAP plays an important role in lipid metabolism by controlling the relative proportions of PA and DAG (27, 47). An imbalance of these intermediates due to a loss of PAP activity

TABLE 1

Strains and plasmids used in this work

Strain or plasmid	Relevant characteristics	Source or Ref.
E. coli strains		
DH5α	F⁻ φ80d*lacZ*ΔM15 Δ (*lacZYA-argF*)U169 *deoR recA1 endA1 hsdR17* (r_k^- m_k^+) *phoA supE44* l⁻ *thi-1 gyrA96 relA1*	Ref. 51
BL21(DE3)pLysS	F⁻ *ompT hsdS_B* (r_B^- m_B^-) *gal dcm* (DE3) pLysS	Novagen
S. cerevisiae strains		
BY4741	*MAT***a** *his3Δ1 leu2Δ0 met15Δ0 ura3Δ0*	Ref. 109
BY4741-app1Δ	*app1Δ::kanMX4* derivative of BY4741	Deletion consortium
W303–1A	*MAT***a** *ade2–1 can1–100 his3–11,15 leu2–3,112 trp1–1 ura3–1*	Ref. 110
GHY63	*app1Δ::natMX4* derivative of W303–1A	This study
GHY57	*pah1Δ::URA3* derivative of W303–1A	Ref. 27
GHY64	*app1Δ::natMX4 pah1Δ::URA3* derivative of W303–1A	This study
TBY1	*dpp1Δ::TRP1/Kan^r lpp1Δ::HIS3/Kan^r* derivative of W303–1A	Ref. 29
GHY65	*app1Δ::natMX4 dpp1Δ::TRP1/Kan^r lpp1Δ::HIS3/Kan^r* derivative of W303–1A	This study
GHY58	*pah1Δ::URA3 dpp1Δ::TRP1/Kan^r lpp1Δ::HIS3/Kan^r* derivative of W303–1A	Ref. 27
GHY66	*app1Δ::natMX4 pah1Δ::URA3 dpp1Δ::TRP1/Kan^r lpp1Δ::HIS3/Kan^r* derivative of W303–1A	This study
Plasmids		
YEp351	Multicopy *E. coli*/yeast shuttle vector with *LEU2*	Ref. 91
pMC102	*APP1* gene inserted into YEp351	This study
pMC102-D281E	*APP1* (D281E) derivative of pMC102	This study
pMC103	*APP1^HA* gene inserted into YEp351	This study
pMC103-D281E	*APP1* (D281E) derivative of pMC103	This study
pET-15b	*E. coli* expression vector with N-terminal His₆ tag fusion	Novagen
pMC101	*APP1* coding sequence inserted into pET-15b	This study

results in cellular abnormalities that include a drastic reduction in TAG abundance and susceptibility to fatty acid-induced lipotoxicity, the misregulation of phospholipid synthesis and an aberrant expansion of the nuclear/endoplasmic reticulum membrane, and defects in lipid droplet formation and vacuole homeostasis (27, 30, 43, 47–49). The Dpp1p and Lpp1p are not involved in *de novo* lipid synthesis that occurs at the endoplasmic reticulum (21, 28, 29). Instead, these enzymes are thought to have roles in lipid signaling by controlling the amounts of PA, DAG pyrophosphate, and lysoPA in the organelles where they reside (21, 26).

A significant amount of Mg^{2+}-dependent PAP activity is still present in the *pah1Δ dpp1Δ lpp1Δ* triple mutant (27). However, unlike Pah1p PAP, this activity is sensitive to inhibition by *N*-ethylmaleimide (27). The enzyme activity is found in both the cytosolic and the membrane fractions of the cell, and its association with the membrane is peripheral in nature (27). Studies to gain insight into the physiological role of the PAP activity have been hampered because the gene encoding the enzyme has yet to be identified. In this work, we purified PAP from the *pah1Δ dpp1Δ lpp1Δ* triple mutant and identified *APP1* as the gene encoding the enzyme. The lack of detectable PAP activity in the *app1Δ pah1Δ dpp1Δ lpp1Δ* quadruple mutant indicated that all PAP activity in yeast is encoded by *APP1*, *PAH1*, *DPP1*, and *LPP1*. Moreover, this work identified the molecular function of the actin patch protein App1p as a PAP enzyme.

EXPERIMENTAL PROCEDURES

Materials

All chemicals were reagent grade. Growth medium supplies were purchased from Difco. Polyvinylidene difluoride membrane, the enhanced chemiluminescence Western blotting detection kit, phenyl-Sepharose CL-4B, MonoQ, and Superdex 200 columns were purchased from GE Healthcare. DE52 (DEAE-cellulose) was purchased from Whatman. Affi-Gel Blue, protein assay reagents, electrophoretic reagents, and protein standards were purchased from Bio-Rad. Radiochemicals

were purchased from PerkinElmer Life Sciences. Bovine serum albumin, phenylmethylsulfonyl fluoride, benzamidine, aprotinin, leupeptin, pepstatin, isopropyl-*β*-D-thiogalactoside, sodium cholate, and Triton X-100 were purchased from Sigma. Lipids were obtained from Avanti Polar Lipids. Silica gel thin-layer chromatography plates were from EM Science. Restriction endonucleases, modifying enzymes, and recombinant VentR DNA polymerase were purchased from New England Biolabs. Plasmid isolation and gel extraction kits and Ni^{2+}-NTA-agarose resin were purchased from Qiagen. Invitrogen was the source of the DNA size standards and the yeast deletion consortium strain collection. The Yeast Maker yeast transformation kit was purchased from Clontech. Stratagene supplied the QuikChange site-directed mutagenesis kit. Nourseothricin (LEXSY NTC) was purchased from Jena Bioscience. Mouse monoclonal anti-HA, and anti-His₆ antibodies were from Roche Applied Science. Anti-App1p antibodies were prepared in rabbits against the C-terminal portion (residues 490–502) of the protein at EZBiolab. Alkaline phosphatase-conjugated goat anti-rabbit IgG antibodies and alkaline phosphatase-conjugated goat anti-mouse IgG antibodies were from Thermo Scientific and Pierce, respectively. Scintillation counting supplies were purchased from National Diagnostics.

Strains and Growth Conditions

The strains used in this work are listed in Table 1. Yeast cells were grown in YEPD medium (1% yeast extract, 2% peptone, 2% glucose) or in synthetic complete medium containing 2% glucose at 30 °C as described previously (50, 51). For selection of yeast cells bearing plasmids, the appropriate amino acids were omitted from synthetic complete medium. Plasmid maintenance/amplifications (strain DH5α) and App1p expression (strain BL21(DE3)pLysS) were performed in *Escherichia coli*. The bacterial cells were grown in LB medium (1% Tryptone, 0.5% yeast extract, 1% NaCl, pH 7.4) at 37 °C, and ampicillin (100 μg/ml) was added to select for the cells carrying plasmid. For growth on solid media, agar plates were prepared with supplementation of either 2% (yeast) or 1.5% (*E. coli*) agar. For

App1p Is a Phosphatidate Phosphatase

App1p PAP purification in yeast, *pah1Δ dpp1Δ lpp1Δ* mutant cells were grown to late exponential phase in YEPD medium at 30 °C. For heterologous expression of His$_6$-tagged App1p, *E. coli* BL21(DE3)pLysS cells bearing pMC101 were grown to $A_{600\,nm} = 0.5$ at 30 °C in 1 liter of LB medium containing ampicillin (100 μg/ml) and chloramphenicol (34 μg/ml). The culture was then incubated for 3 h with 1 mM isopropyl-B-D-thiogalactoside to induce the expression of the PAP enzyme.

DNA Manipulations, Cloning of APP1, and Construction of Plasmids

Standard methods were used to isolate plasmid and genomic DNA and for manipulation of DNA using restriction enzymes, DNA ligase, and modifying enzymes (51). Transformations of *S. cerevisiae* (52) and *E. coli* (51) with DNA/plasmids and PCR reactions (53) followed the standard protocols. The plasmids used in this work are listed in Table 1. The *S. cerevisiae APP1* gene was cloned by PCR. A 3,024-bp DNA fragment that contains the entire coding sequence (1,764 bp) of *APP1*, the 5′-untranslated region (824 bp), and the 3′-untranslated region (436 bp) was amplified from W303-1A genomic DNA (forward, 5′-GATTATAAGCTTAACTGACACCCATATCGCTTGACCC-3′; reverse, 5′-GGTCAATATACGTGCATCTAGAAGGCCTTTCCCGAC-3′). The *APP1* DNA fragment was digested with HindIII/XbaI and inserted into plasmid YEp351 at the same restriction enzyme sites. The multicopy plasmid containing *APP1* was named pMC102. The *APP1* gene was used to construct *APP1^HA*, in which the sequence for the HA epitope (YPYDVPDYA) was located after the start codon. The 854-bp (forward, 5′-GATTATAAGCTTAACTGACACCCATATCGCTTGACCC-3′; reverse, 5′-AGCGTAGTCTGGGACGTCGTATGGGTACATCTTTTTATTCCTTCTCCAAAGCAATTTTTTCCCCC-3′) and 2,224-bp (forward, 5-TACCCATACGACGTCCCAGACTACGCTAATAGTCAAGGTTACGATGAAAGCTCTTCCTCTACTGC-3′; reverse, 5′-GGTCAATATACGTGCATCTAGAAGGCCTTTCCCGAC-3′) *APP1* DNA fragments that contain the HA tag at the 3′ and 5′ ends, respectively, were amplified by PCR. These PCR products containing 27-bp overlapping ends were combined by overlap extension PCR. The combined 3,051-bp DNA was then amplified, digested with HindIII and XbaI, and inserted into YEp351 at HindIII/XbaI sites. The multicopy plasmid containing *APP1^HA* was named pMC103. Plasmids pMC102-D281E and pMC103-D281E were produced by PCR-mediated site-directed mutagenesis with the codon change of GAT to GAA. The nucleotide change in the *APP1* and *APP1^HA* alleles was confirmed by DNA sequencing. For expression of *APP1* in *E. coli*, its coding sequence (except the first nucleotide) was amplified by PCR from genomic DNA template (forward, 5′-TGAATAGTCAAGGTTACGATGAAAGCTCTTCC-3′; reverse, 5′-TAATCCTCGAGTTAGTTTGAATACTTCTCCCTAATTCTGCG-3′). The 1,774-bp PCR product was digested with XhoI, and the vector pET-15b was digested with NdeI, filled with Klenow, and digested with XhoI. The blunt cohesive end PCR products were inserted into pET-15b at NdeI (Klenow)/XhoI sites. The plasmid bearing His$_6$-tagged *APP1* was named pMC101.

Construction of the app1Δ Mutant and Its Derivatives

The *app1Δ* mutation in the wild type strain W303-1A and in the *dpp1Δ lpp1Δ* mutant strain TBY1 was generated by one-step gene replacement (54). The strains were transformed with the 1,219-bp disruption cassette (*app1Δ::natMX4*) that had been amplified from pAG25 (EUROSCARF) (forward, 5′-AGTTCCGTCAAAGGGGGGAAAAAATTGCTTTGGGAGAAGGAATAAAAAGATGACATGGAGGCCCAGAATACCC-3′; reverse, 5′-TATACAATTTTTAAACTCCCTCCCGATGTATATAAATAACAGTGTATTTACAGTATAGCGACCAGCATTCAC-3′). Yeast transformants were selected on YEPD medium containing 100 μg/ml nourseothricin, and the *app1Δ* mutation in the nourseothricin-resistant cells was confirmed by PCR amplification of the 1,217-bp fragment from genomic DNA (forward, 5′-AGGGGGAAAAAATTGCTTTGGA-3′; reverse, 5′-ATACAATTTTTAAACTCCCTCCCG-3′). The *pah1Δ* mutation in the *app1Δ* mutant strain GHY63 and the *app1Δ dpp1Δ lpp1Δ* mutant strain GHY65 was generated by one-step gene replacement as described previously (27).

Partial Purification of App1p PAP from S. cerevisiae

The *pah1Δ dpp1Δ lpp1Δ* mutant strain GHY58 (27) was used to purify PAP activity that is not encoded by the *PAH1* (27), *DPP1* (28), or *LPP1* (29) gene. All steps were performed at 8 °C.

Step 1: Preparation of Cell Extract—The *pah1Δ dpp1Δ lpp1Δ* triple mutant cells were harvested in the late exponential phase, and cells were resuspended in buffer A (50 mM Tris-HCl (pH 7.5), 0.3 M sucrose, 10 mM 2-mercaptoethanol, 1 mM Na$_2$EDTA, 0.5 mM phenylmethanesulfonyl fluoride, 1 mM benzamide, 5 μg/ml aprotinin, 5 μg/ml leupeptin, 5 μg/ml pepstatin). Cells (200 g, wet weight) were disrupted with glass beads (0.5-mm diameter) using a Biospec Products BeadBeater as described previously (55). The cell lysate was centrifuged at 1,500 × *g* for 10 min to remove unbroken cells and glass beads. Protein concentration was estimated by the method of Bradford (56) using bovine serum albumin as the standard.

Step 2: Preparation of Crude Mitochondria—Crude mitochondria were collected from the cell extract by centrifugation at 32,000 × *g* for 10 min (57).

Step 3: Preparation of NaCl Extract—Mitochondria were suspended in buffer A containing 1 M NaCl to a final protein concentration of 10 mg/ml. The suspension was centrifuged at 32,000 × *g* for 10 min to remove salt-unextractable proteins from mitochondrial membranes. The supernatant containing the salt-extracted proteins was then dialyzed overnight against buffer B (50 mM Tris-HCl (pH 7.5), 1 mM MgCl$_2$, 10 mM 2-mercaptoethanol, 1 mM phenylmethylsulfonyl fluoride) containing 0.5% sodium cholate. Sodium cholate was added to buffer B to prevent the precipitation of PAP that occurred after the removal of salt from the enzyme preparation.

Step 4: DE52 Chromatography—A DE52 column (1.5 × 7 cm) was equilibrated with buffer B containing 0.5% sodium cholate. The enzyme preparation from the previous step was applied to the column at a flow rate of 40 ml/h, and the column was washed with 5 column volumes of buffer B plus 0.5% sodium cholate followed by elution of the enzyme in 5-ml fractions with

10 column volumes of a linear NaCl gradient (0–0.5 M) in the same buffer. The peak of PAP activity eluted at 0.2 M NaCl.

Step 5: Affi-Gel Blue Chromatography—An Affi-Gel blue column (1.5 × 5 cm) was equilibrated with buffer B containing 0.5% sodium cholate and 0.2 M NaCl. The DE52-purified enzyme was applied to the column at a flow rate of 60 ml/h. The column was washed with 5 column volumes of buffer B containing 0.5% sodium cholate and 0.5 M NaCl. PAP activity was then eluted in 3-ml fractions with 12 column volumes of a linear gradient of NaCl (0.5–3.0 M) in buffer B containing 0.2% sodium cholate. The peak of activity eluted at a NaCl concentration of 1.3 M.

Step 6: Phenyl-Sepharose Chromatography—A phenyl-Sepharose (0.8 × 2 cm) column was equilibrated with buffer B containing 0.2% sodium cholate and 3 M NaCl. The Affi-Gel Blue-purified enzyme was made to contain 3 M NaCl and then applied to the column under gravity flow. The column was first washed with 10 column volumes of the equilibration buffer and then washed with 10 column volumes of the buffer without NaCl. PAP activity was then eluted in 1-ml fractions with 1% Triton X-100 in buffer B. Hereafter, the PAP activity was made soluble with Triton X-100 instead of sodium cholate.

Step 7: MonoQ Chromatography—A MonoQ column (0.5 × 5 cm) was equilibrated with buffer B containing 0.5% Triton X-100. The phenyl-Sepharose-purified enzyme was applied to the column; the column was then washed with 5 column volumes of buffer B containing 0.5% Triton X-100 followed by elution of PAP in 1-ml fractions with 20 column volumes of a linear NaCl gradient (0–1 M) at a flow rate 24 ml/h. The peak of activity was eluted at NaCl concentration of 0.5 M.

Step 8: Superdex 200 Chromatography—A gel filtration Superdex 200 column (1 × 30 cm) was equilibrated with buffer C containing 0.5 M NaCl and 0.5% Triton X-100. The MonoQ-purified enzyme was applied to the column at a flow rate of 40 ml/h. The enzyme was then eluted in 0.5-ml fractions with 1 column volume of the same buffer.

Purification of His$_6$-tagged App1p PAP from E. coli

All steps were performed at 8 °C. *E. coli* cells expressing His$_6$-tagged App1p were suspended in 20 ml of 20 mM Tris-HCl (pH 8.0) buffer containing 0.5 M NaCl, 5 mM imidazole, and 1 mM phenylmethylsulfonyl fluoride. Cells were disrupted by a freeze-thawing cycle and by two passes through a French press at 20,000 p.s.i. Unbroken cells and cell debris were removed by centrifugation at 12,000 *g* for 30 min at 4 °C. The supernatant (cell lysate) was gently mixed with 2 ml of 50% slurry of Ni^{2+}-NTA-agarose for 2 h. The Ni^{2+}-NTA-agarose/enzyme mixture was packed in a 10-ml column and washed with 20 ml of 20 mM Tris-HCl (pH 8.0) buffer containing 0.5 M NaCl, 45 mM imidazole, 10% glycerol, and 7 mM 2-mercaptoethanol. His$_6$-tagged App1p was eluted from the column in 1-ml fractions with 20 mM Tris-HCl (pH 8.0) buffer containing 0.5 M NaCl, 250 mM imidazole, 10% glycerol, and 7 mM 2-mercaptoethanol. Purified enzyme preparations were stored at −80 °C.

PAP Assay

PAP activity was measured for 20 min by following the release of water-soluble [^{32}P]P$_i$ from chloroform-soluble [^{32}P]PA (5,000 cpm/nmol) at 30 °C as described previously (58). The [^{32}P]PA substrate was synthesized enzymatically from DAG and [γ-^{32}P]ATP with *E. coli* DAG kinase (58). The reaction mixture contained 50 mM Tris-HCl buffer (pH 7.5), 1 mM MgCl$_2$, 0.2 mM PA, 2 mM Triton X-100, 10 mM 2-mercaptoethanol, and enzyme protein in a total volume of 0.1 ml. Enzyme assays were conducted in triplicate, and the average standard deviation of the assays was ± 5%. All reactions were linear with time and protein concentration. A unit of enzyme activity was defined as the amount of enzyme that catalyzed the formation of 1 nmol of product per minute.

SDS-PAGE and Western Blot Analysis

SDS-PAGE (59) using 10% slab gels and Western blotting (60, 61) using polyvinylidene difluoride membrane were performed as described previously. Proteins in polyacrylamide gels were visualized by staining with Coomassie Blue R250. The anti-HA, anti-His$_6$, and anti-App1p antibodies were used at dilutions of 1:500, 1:5000, and 1:5000, respectively. Alkaline phosphatase-conjugated goat anti-mouse IgG antibodies and goat anti-rabbit IgG antibodies were used at a dilution of 1:5,000. Immune complexes were detected using the enhanced chemiluminescence Western blotting detection kit. Fluorimaging was used to acquire images from Western blots.

Identification of Proteins by Liquid Chromatography/Tandem Mass Spectrometry

An SDS-polyacrylamide gel slice containing proteins purified through the Superdex 200 chromatography step was subjected to trypsin digestion (62) followed by liquid chromatography/tandem mass spectrometry using a Thermo Fisher Scientific LTQ Orbitrap Velos instrument (63). The spectra were searched against the Swiss-Prot yeast database using the MASCOT (V.2.3) search engine (62). This work was performed at the Center for Advanced Proteomics Research facility of the University of Medicine and Dentistry of New Jersey (Newark, NJ).

Labeling and Analysis of Lipids

Steady-state labeling of phospholipids and neutral lipids with [^{32}P]P$_i$ and [2-^{14}C]acetate, respectively, was performed as described previously (27). Lipids were extracted from labeled cells by the method of Bligh and Dyer (64). Phospholipids were analyzed by two-dimensional thin-layer chromatography on silica gel plates using chloroform/methanol/ammonium hydroxide/water (45:25:2:3, v/v) as the solvent system for dimension one and chloroform/methanol/glacial acetic acid/water (32:4:5:1, v/v) as the solvent system for dimension two (65). Neutral lipids were analyzed by one-dimensional thin-layer chromatography on silica gel plates using the solvent system hexane/diethyl ether/glacial acetic acid (40:10:1, v/v) (66). The identity of the labeled lipids on TLC plates was confirmed by comparison with standards after exposure to iodine vapor. Radiolabeled lipids were visualized by phosphorimaging analysis. The relative quantities of labeled lipids were analyzed using ImageQuant software.

TABLE 2

Partial purification of App1p PAP from *S. cerevisiae*

PAP was purified from *pah1Δ dpp1Δ lpp1Δ* mutant cells as described under "Experimental Procedures." The data are based on starting with 200 g (wet weight) of cells.

| Purification step	Total units	Protein	Specific activity	Yield	Purification
	nmol/min	*mg*	*units/mg*	*%*	*-fold*
Cell extract	3,237	4,625	0.7	100	1
Mitochondria	2,200	628	3.5	68	5
NaCl extract	1,745	346	5	54	7
DE52	1,053	65	16	33	23
Affi-Gel Blue	770	20	39	24	56
Phenyl-Sepharose	545	4	137	17	196
MonoQ	300	0.9	330	9	471
Superdex 200	150	0.1	1,500	5	2,143

Analyses of Data

Statistical analyses were performed with SigmaPlot software. The *p* values < 0.05 were taken as a significant difference.

RESULTS

PAP Activity in the pah1Δ dpp1Δ lpp1Δ Triple Mutant Is Encoded by the APP1 Gene—The *pah1Δ dpp1Δ lpp1Δ* triple mutant, which does not contain PAP encoded by known genes (*i.e. PAH1*, *DPP1*, and *LPP1*), was used to purify the unknown PAP enzyme. The PAP activity in the triple mutant was associated with the cytosolic (0.7 ± 0.3 nmol/min/mg), microsomal (1 ± 0.1 nmol/min/mg), and mitochondrial (5 ± 0.3 nmol/min/mg) fractions. The PAP specific activity was enriched 5-fold in the mitochondrial fraction over the cell extract, and accordingly, this fraction was used as the source of enzyme. PAP activity was dissociated from mitochondrial membranes with 1 M NaCl followed by dialysis for desalting and chromatography with DE52, Affi-Gel Blue, phenyl-Sepharose, MonoQ, and Superdex 200. We noted the precipitation of PAP activity upon the removal of salt, and thus, sodium cholate or Triton X-100 was included in the chromatography buffers to maintain its solubility. The presence of salt also stabilized PAP activity. The Superdex 200 step afforded the greatest enrichment (4.5-fold) in specific activity (Table 2). The elution profiles of PAP activity and protein and an SDS-PAGE analysis indicated that the enzyme preparation was not pure (Fig. 1). Attempts to further purify the enzyme were unsuccessful because the PAP activity was labile. Overall, the enzyme was purified 2,143-fold over the cell extract to a final specific activity of 1,500 nmol/min/mg with an activity yield of 5% (Table 2).

The peak of PAP activity that emerged from the Superdex 200 column correlated with the enrichment of a minor protein band that migrated just above the size of the 50-kDa molecular mass marker (Fig. 1, *fraction 27*, indicated by the *asterisk*). An SDS-polyacrylamide gel slice containing this band was subjected to trypsin digestion followed by the analysis of peptides by liquid chromatography-mass spectrometry. This analysis yielded a few proteins of unknown function that upon further analysis (*e.g.* expression and purification in *E. coli*) showed no PAP activity. This indicated that the PAP enzyme in the preparation was very low in abundance. Accordingly, we used more sensitive liquid chromatography-tandem mass spectrometry to detect low abundance proteins. This analysis revealed that the enzyme preparation contained 112 proteins (or proteolytic fragments thereof). From the list, we focused on those proteins
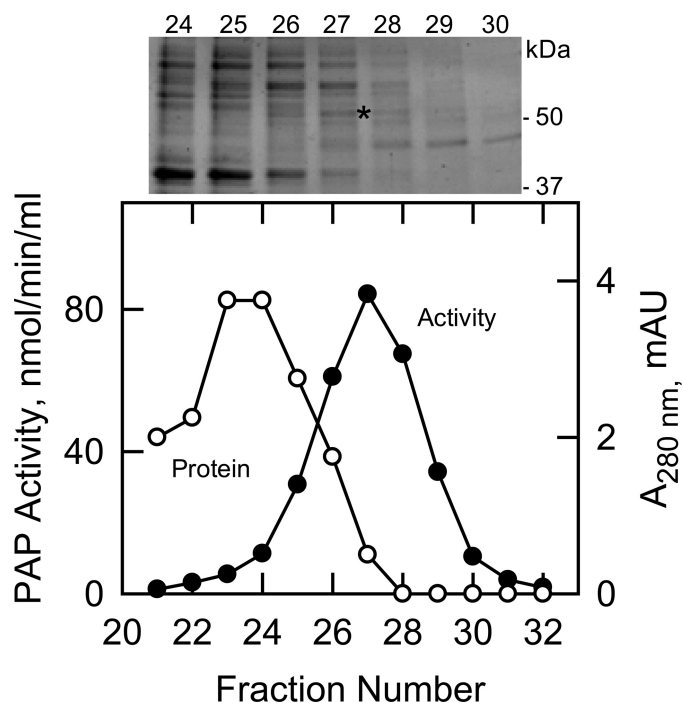

FIGURE 1. **Elution profiles of PAP activity and protein after chromatography with Superdex 200 and SDS-PAGE of the purified enzyme.** The MonoQ-purified PAP enzyme preparation was subjected to chromatography with Superdex 200. Fractions were collected and assayed for PAP activity (●) and protein (○). Fractions 24–30 were subjected to SDS-PAGE followed by staining with Coomassie Blue (*above plot*). The positions of electrophoresis molecular mass standards are indicated in the figure. The band derived from fraction 27 that was used for protein sequencing is indicated by the *asterisk*. *mAU*, milliabsorbance units.

with unknown molecular function that possessed a phosphatase motif. We also considered proteins that are thought to be involved in phospholipid synthesis. Based on these criteria, we analyzed cell extracts from 20 mutants from the yeast deletion strain collection for a loss in PAP activity. Of the mutants, only *app1Δ* exhibited a 30% decrease in PAP activity when compared with the wild type parental strain. These data indicated that the PAP activity might be directed by the *APP1* gene.

The acronym *APP1* stands for <u>a</u>ctin <u>p</u>atch <u>p</u>rotein (67) because App1p is a component of cortical actin patches and interacts with endocytic proteins (67–75) (Fig. 2). Pfam analysis indicated that App1p consisting of 587 amino acids in length (66.1 kDa) contains a region with weak sequence similarity to a haloacid dehalogenase-like domain (76) (Fig. 2). Contained within this domain is a DXDX(T/V) (residues 281–285) catalytic motif that is present in the superfamily of Mg^{2+}-dependent phosphatase enzymes (77) that include yeast Pah1p and mammalian lipin PAP enzymes (27, 78). App1p also contains several PXXP motifs (Fig. 2) that are important for interactions with proteins that possess SH3 domains (79, 80).

To prove that *APP1* encodes PAP, we used heterologous overexpression of *APP1* in *E. coli*. The *S. cerevisiae APP1* coding sequence was amplified by PCR and inserted into plasmid pET-15b for the isopropyl-β-D-thiogalactoside-inducible expression of His$_6$-tagged protein. The purified His$_6$-tagged App1p migrated upon SDS-PAGE at the expected size of ~68 kDa (Fig. 3*A*). In addition, the purified protein was confirmed by immune reaction with antibodies directed against the His$_6$ epitope
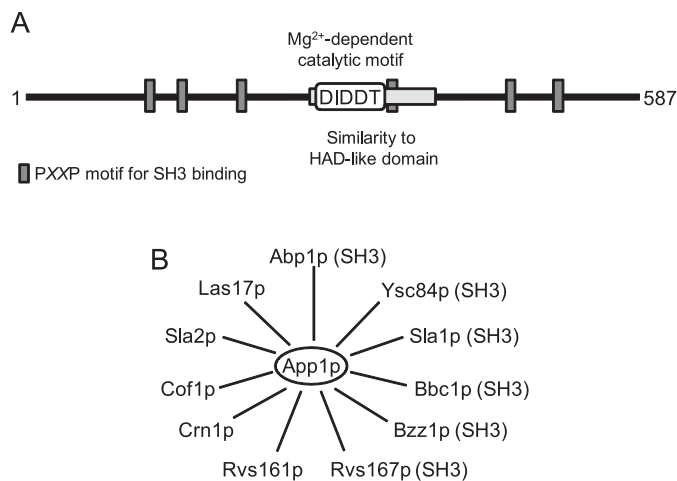
FIGURE 2. **Motifs in App1p and its interacting endocytic cortical actin patch proteins.** *A*, the diagram shows a linear representation of App1p with the approximate positions of the region that has similarity to a haloacid dehalogenase (*HAD*)-like domain (76), the D*X*D*X*(T/V) catalytic motif, and the P*XX*P motif for SH3 binding. *B*, the diagram shows that App1p interacts with the endocytic proteins Abp1p (69–73), Bbc1p (70, 73), Bzz1p (70, 73, 74), Cof1p (69), Crn1p (67), Las17p (75), Rvs161p (67, 68, 70, 73, 74), Rvs167p (67, 68, 70, 73, 74), Sla1p (67, 73), Sla2p (67), and Ysc84p (70, 73). The proteins that possess SH3 binding domains are indicated by the *parentheses* after the name.
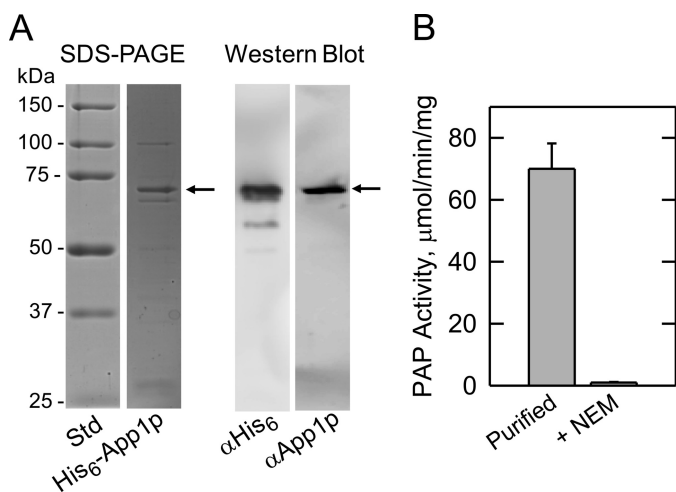
FIGURE 3. **SDS-PAGE and Western blot analysis of His$_6$-tagged App1p purified from *E. coli* and the PAP activity of the purified enzyme.** *A*, molecular mass standards (*Std*) and His$_6$-tagged App1p (1 µg) purified from *E. coli* were subjected to SDS-PAGE and stained with Coomassie Blue (*left*). The purified His$_6$-tagged App1p (samples of 1 µg and 1 ng, respectively) was subjected to Western blot analysis using a 1:5000 dilution of anti-His$_6$ (*αHis$_6$*) and anti-App1p (*αApp1p*) antibodies, respectively (*right*). *B*, PAP activity of purified His$_6$-tagged App1p measured in the absence and presence of 20 mM *N*-ethylmaleimide (*NEM*). The data in *A* were representative of two experiments, whereas the data in *B* were the average of three experiments ± S.D. (*error bars*).

and against a peptide sequence found at the C-terminal portion of App1p (Fig. 3*A*). The purified protein catalyzed the Mg^{2+}-dependent PAP reaction, and the addition of 10 mM Na$_2$EDTA abolished PAP activity. Unlike the Mg^{2+}-dependent Pah1p PAP, App1p enzyme activity was sensitive to inhibition by *N*-ethylmaleimide (Fig. 3*B*). That App1p expressed in *E. coli* exhibits PAP activity also indicated that a posttranslational modification that might occur in yeast is not essential for enzyme activity.

PAP Activity Is Affected by the app1Δ pah1Δ dpp1Δ lpp1Δ Mutations and by the APP1(D281E) Mutation—We constructed a variety of isogenic mutants where the *app1Δ* muta-
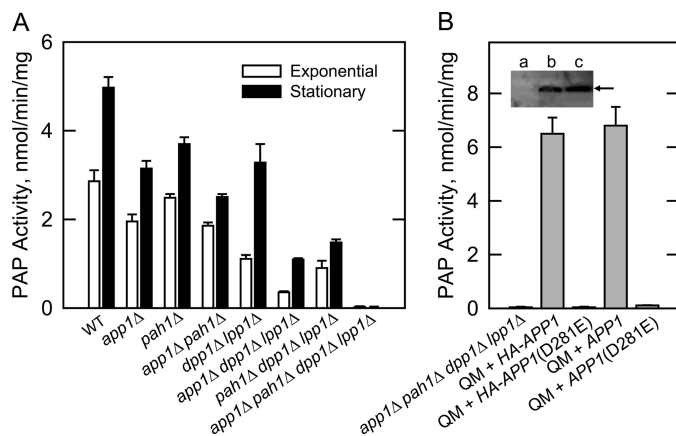

FIGURE 4. **Effects of the *app1Δ* mutation, *APP1* overexpression, and *APP1*(D281E) mutation on PAP activity.** *A*, PAP activity was measured in cell extracts prepared from the indicated mutants grown to the exponential and stationary phases of growth. *B*, cell extracts were prepared from the indicated cells at the exponential phase of growth and assayed for PAP activity. *Inset*, samples (50 µg protein) of the cell extracts were subjected to Western blot using a 1:500 dilution of anti-HA antibodies. Lanes *a*, *b*, and *c* correspond to the *app1Δ pah1Δ dpp1Δ lpp1Δ* quadruple mutant (*QM*), and the QM mutant overexpressing *HA-APP1* and *HA-APP1*(D281E), respectively. The *arrow* indicates the position of HA-tagged App1p. The activity data shown in *A* and *B* were the average of three experiments ± S.D. (*error bars*), whereas the Western blot shown in *B* is representative of three experiments.

tion was combined with mutations of the other PAP genes in *S. cerevisiae* (Table 1). In this manner, we could determine the contribution of *APP1* and the other PAP genes to the total PAP activity in yeast. In wild type cells, PAP activity is known to increase in the stationary phase of growth (81), and accordingly, the effect of the mutations was examined in both exponential and stationary phase cells (Fig. 4*A*). The *APP1* gene accounted for 32 and 37% of the PAP activity in cell extracts of exponential and stationary phase cells, respectively. The *PAH1*-encoded enzyme accounted for 11 and 24% of the PAP activity in exponential and stationary phases, respectively. In the exponential phase, *DPP1* and *LPP1* accounted for 60% of the total PAP activity. A comparison of the activities from *app1Δ pah1Δ* and *dpp1Δ lpp1Δ* double mutants and from the *app1Δ dpp1Δ lpp1Δ* and *pah1Δ dpp1Δ lpp1Δ* triple mutants indicated that *APP1* and *PAH1* were primarily responsible for the induced expression of PAP activity in the stationary phase. The induced expression of *DPP1*-encoded PAP activity in stationary phase cells is governed by inositol (82), a phospholipid precursor that was not supplemented to the growth medium in this work. Finally, the lack of detectable PAP activity in the *app1Δ pah1Δ dpp1Δ lpp1Δ* quadruple mutant indicated that all PAP activity (*i.e.* Mg^{2+}-dependent and Mg^{2+}-independent) in *S. cerevisiae* was attributed to *APP1*, *PAH1*, *DPP1*, and *LPP1* (Fig. 4*A*).

APP1 and *HA-APP1* versions were expressed on a multicopy plasmid in the *app1Δ pah1Δ dpp1Δ lpp1Δ* quadruple mutant, and cell extracts were prepared for the measurement of PAP activity. The PAP-deficient mutant expressing these genes exhibited PAP activities of 6.8 ± 0.7 and 6.5 ± 0.6 nmol/min/mg, respectively (Fig. 4*B*). This corresponded to about a 10-fold overproduction of activity when compared with that found in the *pah1Δ dpp1Δ lpp1Δ* triple mutant (Fig. 4*A*). That both versions of *APP1* directed the same level of activity indicated that the HA epitope did not compromise enzyme activity. The first
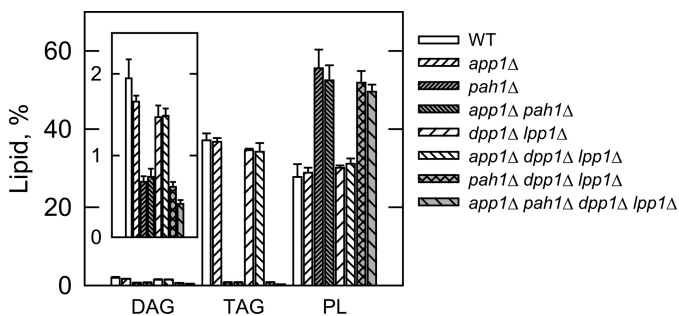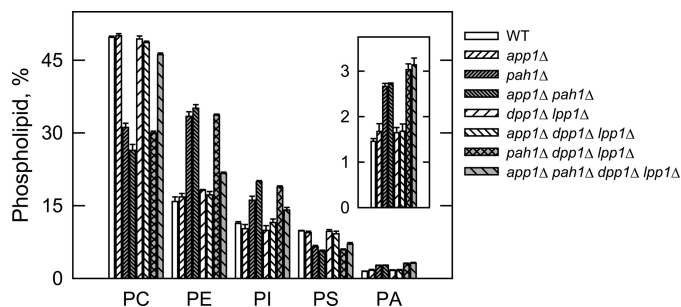
FIGURE 5. **Effects of the PAP gene mutations on DAG, TAG, and total phospholipids.** The indicated cells were grown to the stationary phase of growth in the presence of $[2\text{-}^{14}C]$acetate (1 μCi/ml). Lipids were extracted and separated by one-dimensional TLC, and the images were subjected to ImageQuant analysis. The percentages shown for the individual lipids were normalized to the total ^{14}C-labeled chloroform-soluble fraction, which also contained sterols, fatty acids, and unidentified neutral lipids. Each data point represents the average of three experiments $\pm$ S.D. (*error bars*). *PL*, phospholipids.

FIGURE 6. **Effects of the PAP gene mutations on phospholipid composition.** The indicated cells were grown to the exponential phase of growth in the presence of $[^{32}P]P_i$ (10 μCi/ml). Phospholipids were extracted and separated by two-dimensional TLC, and the images were subjected to ImageQuant analysis. The percentages shown for the individual phospholipids were normalized to the total ^{32}P-labeled chloroform-soluble fraction that included sphingolipids and unidentified phospholipids. Each data point represents the average of three experiments $\pm$ S.D. (*error bars*). Abbreviations: *PC*, phosphatidylcholine; *PE*, phosphatidylethanolamine; *PI*, phosphatidylinositol; *PS*, phosphatidylserine.

conserved aspartate residue in the DIDDT sequence in App1p was mutated to glutamate by site-specific mutagenesis. Glutamate was chosen to replace aspartate to conserve the charge of the amino acid at this position, and thus, minimize a structural change in the enzyme. The D281E mutation abolished the overexpressed PAP activity directed by the *APP1* and *HA-APP1* genes (Fig. 4*B*). An immunoblot analysis using anti-HA antibodies showed that the D281E mutation in the HA-tagged version of App1p did not affect the expression of the enzyme (Fig. 4*B*, *inset*). These data indicated that the DIDDT sequence in App1p is responsible for its PAP catalytic function.

Effects of the app1Δ pah1Δ dpp1Δ lpp1Δ Mutations on Lipid Composition—The PAP deletion mutants were used to determine the contribution of *APP1*, *PAH1*, *DPP1*, and *LPP1* to lipid composition. In the first set of experiments, wild type and mutant cells were labeled to steady state with $[2\text{-}^{14}C]$acetate to analyze DAG, TAG, and total phospholipids. Cells were grown to the stationary phase (the growth phase when DAG and TAG are most affected (27)), and lipids were extracted and then analyzed by one-dimensional TLC. When compared with the *pah1Δ* mutation, the *app1Δ* and *dpp1Δ lpp1Δ* mutations did not have a significant effect on the relative amounts of DAG, TAG, and total phospholipids (Fig. 5). Moreover, alterations in lipid composition observed in the double, triple, and quadruple mutants were attributed to the *pah1Δ* mutation (Fig. 5). These results indicate that of the genes encoding PAP in *S. cerevisiae*, *PAH1* is responsible for the synthesis of TAG and the regulation of phospholipid synthesis. In the second set of experiments, the wild type and mutant cells were labeled to steady state with $[^{32}P]P_i$ to analyze the composition of individual phospholipids. The phospholipids were extracted from exponential phase cells (the growth phase when phospholipid composition is most affected (27)) and analyzed by two-dimensional TLC. The relative amounts of the major phospholipids phosphatidylcholine, phosphatidylethanolamine, phosphatidylinositol, phosphatidylserine, and the precursor PA were not affected by the *app1Δ* and *dpp1Δ lpp1Δ* mutations (Fig. 6). The relative amounts of these phospholipids, however, were affected by the *pah1Δ* mutation alone and in combination with the *app1Δ* and *dpp1Δ lpp1Δ* mutations (Fig. 6). As described previously (27), the *pah1Δ* mutation caused decreases in the amounts of phos-

phatidylcholine (37%) and phosphatidylserine (33%) and increases in the amounts of phosphatidylethanolamine (108%), phosphatidylinositol (42%), and PA (86%). Interestingly, when combined with the *pah1Δ dpp1Δ lpp1Δ* mutations, the *app1Δ* mutation reversed the effect of the *pah1Δ* mutation on the composition of phosphatidylcholine and phosphatidylethanolamine. The reason for this change is unclear.

The app1Δ Mutant Does Not Exhibit Obvious Phenotypes— We noted that the *app1Δ* mutant in the BY4741 genetic background exhibited slower growth on synthetic medium and was sensitive to elevated temperature (*i.e.* 37 °C). It is known that the BY4741 strain has more stringent growth requirements when compared with other strains used by the yeast research community (83). Accordingly, the growth requirements of the *app1Δ* mutant were also examined in the W303-1A genetic background. This analysis showed that the *app1Δ* mutation did not cause obvious growth defects. In addition, no striking phenotypes (*e.g.* changes in cellular morphology, respiratory deficiency, salt sensitivity) were identified. In striking contrast, the *pah1Δ* mutant exhibits a slow growth phenotype, is temperature-sensitive in several genetic backgrounds, and exhibits defects in cellular morphology (27, 43, 48, 49, 84). None of these phenotypes were complemented by the expression of *APP1*, substantiating that App1p and Pah1p PAP activities have distinct functions in lipid metabolism and cell physiology.

DISCUSSION

PAP is generally recognized as an important enzyme in eukaryotic organisms because its substrate PA and product DAG play important roles in the synthesis of TAG and phospholipids and in other aspects of cell physiology (*e.g.* transcription, lipid signaling, and vesicular trafficking) (1–20). Two basic types of PAP activity are found in eukaryotic organisms: an activity that is dependent on Mg^{2+} and an activity that is not dependent on Mg^{2+} or any other divalent cation (21, 22, 74). Mg^{2+}-dependent PAP activity is governed by a DXDX(T/V) catalytic motif (77), whereas Mg^{2+}-independent activity is directed by a three-domain catalytic motif consisting of the sequences KX_6RP, PSGH, and SRX_5HX_3D (31). In the yeast *S. cerevisiae*, the Mg^{2+}-dependent PAP is encoded by *PAH1*

(27), whereas the Mg^{2+}-independent type of the enzyme is encoded by *DPP1* (28) and *LPP1* (29). The *pah1Δ dpp1Δ lpp1Δ* triple mutant lacking the known Mg^{2+}-dependent and Mg^{2+}-independent PAP enzymes still possesses the Mg^{2+}-dependent activity that is sensitive to inhibition by *N*-ethylmaleimide (27), and the identity of the gene(s) encoding this activity was the focus of this work.

APP1 was identified through a reverse genetics approach using protein sequence information derived from the PAP enzyme isolated from the *pah1Δ dpp1Δ lpp1Δ* triple mutant. Obtaining App1p sequence information was not straightforward. The PAP activity was labile in the absence of high salt, which comprised the effectiveness of chromatography steps that required low salt for enzyme binding (*e.g.* ion exchange chromatography). Although the eight-step purification scheme resulted in a 2,143-fold enrichment in PAP specific activity, it did not result in a homogeneous enzyme preparation that could facilitate unequivocal protein sequence determination. Although the sensitive liquid chromatography/tandem mass spectrometry technology yielded many protein candidates, it allowed us to identify App1p that was present in very low abundance. In the end, the collective data (*e.g.* reduction of PAP activity in the *app1Δ* mutant, the *APP1*-directed overexpression of PAP activity in the *app1Δ pah1Δ dpp1Δ lpp1Δ* quadruple mutant, and the heterologous expression of App1p PAP activity in *E. coli*) provided a conclusive level of evidence that *APP1* is the structural gene encoding a PAP enzyme in *S. cerevisiae*.

Efforts to identify *APP1* by informatics and by genetic approaches were unsuccessful. For example, a protein BLAST search using Pah1p as the query did not identify App1p or any other homologs in the *Saccharomyces* genome database. A BLAST search against higher eukaryotic organism databases identified mammalian lipin proteins, but this was expected because a BLAST search with mouse lipin-1 as the query identifies *S. cerevisiae* Pah1p (78). Likewise, a BLAST search using App1p as the query does not identify Pah1p or the mammalian lipins. Instead, the BLAST search identifies App1p homologs only found in fungi. A synthetic genetic array screen using the *pah1Δ* mutant in combination with the *cho2Δ* and *opi3Δ* mutations defective in the phosphatidylethanolamine methylation steps of phosphatidylcholine synthesis via the CDP-DAG pathway (85, 86) has also been performed.[3] The rationale for this analysis was that the loss of a gene encoding PAP in combination with the loss of Pah1p causes lethality due to a lack of DAG production required for the synthesis of phosphatidylcholine via the Kennedy pathway (85, 86). The genetic screen, however, did not lead to the identification of *APP1*,[3] indicating that the cellular functions of App1p and Pah1p do not overlap with each other with respect to lipid synthesis. This assertion was further supported by the fact that *APP1* did not complement phenotypes (*e.g.* temperature sensitivity) exhibited by the *pah1Δ* mutant and that the analysis of cells possessing the *app1Δ* mutation alone and in combination with mutations for other known PAP genes indicated that only Pah1p PAP was involved in *de novo* lipid synthesis.

Although there is essentially no sequence homology between App1p and Pah1p, both enzymes possess the canonical D*X*D*X*(T/V) catalytic motif that is typical of Mg^{2+}-dependent phosphatase enzymes (77). For Pah1p, its DIDGT catalytic sequence is contained within the haloacid dehalogenase-like domain similar to that found in the mammalian lipin PAP enzymes (21, 23, 78). However, the haloacid dehalogenase-like domain is not found in App1p, but instead, it contains a conserved domain found only in fungi that has overlapping regions that show weak sequence similarity to the haloacid dehalogenase-like domain found in Pah1p and lipin (76). It is within this domain that the App1p DIDDT sequence is found (Fig. 2), and indeed, the D281E mutation abolished PAP activity, confirming this to be the catalytic sequence.

PAP enzymes isolated from *S. cerevisiae* are known to have molecular masses of 91 kDa (Mg^{2+}-dependent) (87), 75 kDa (Mg^{2+}-dependent) (88), 45 kDa (Mg^{2+}-dependent) (89), and 34 kDa (Mg^{2+}-independent) (34). Protein sequence information has confirmed that the 91-kDa enzyme is a proteolysis product of Pah1p (27) and that the 34-kDa enzyme is Dpp1p (28). Lpp1p PAP was identified based on its sequence homology with Dpp1p (29). The identity of the genes encoding the 75- and 45-kDa forms of PAP has been an enigma. Although the basic enzymological properties of these enzymes are similar, the 75-kDa enzyme is soluble, whereas the 45-kDa enzyme is associated with mitochondria (88, 89). Because of the differences in size and location, it has been assumed that the 75- and 45-kDa PAP enzymes are encoded by different genes. Based on the result that no detectable PAP activity was present in the *app1Δ pah1Δ dpp1Δ lpp1Δ* quadruple mutant, we hypothesize that the 75-kDa PAP was the soluble form of App1p and that the 45-kDa PAP was a proteolytic fragment of App1p bound to mitochondrial membranes. Unfortunately, this hypothesis cannot be addressed because preparations of the 75- and 45-kDa PAP enzymes are no longer available. Obviously, the protein used for sequence analysis in this study was a proteolytic fragment of App1p.

The PAP enzymes in *S. cerevisiae* are found in different cellular locations and play diverse roles in cell physiology (74). Pah1p is a cytosolic enzyme that associates with and functions at the nuclear/endoplasmic reticulum membrane to regulate the synthesis of TAG and membrane phospholipids (21, 22, 27, 42, 74). Dpp1p and Lpp1p, respectively, are thought to control the signaling functions of PA, DAG pyrophosphate, and lysoPA in vacuole and Golgi membranes (21, 22, 28, 29, 34, 44–46, 74, 90). Like Pah1p, App1p is a cytosolic protein (46) that associates with membranes, but the role this PAP plays in cell physiology is not yet clear.

The formation of endocytic vesicles in *S. cerevisiae* involves a series of processes that include actin patch assembly, actin polymerization, and changes in membrane structure and curvature (75, 92). These processes involve numerous endocytic proteins, and App1p is known to physically interact with many of them (67–75) (Fig. 2). Although these interactions have yet to be studied in detail, the presence of proline-rich regions (P*XX*P motifs) in App1p suggests interactions with SH3 domains of Abp1p, Ysc84p, Sla1p, Bbc1p, Bzz1p, and Rvs167p (79, 80). App1p interactions with proteins that do not possess SH3

---

[3] C. R. McMaster, personal communication.

domains (*e.g.* Las17p, Sla2p, Cof1p, Crn1p, and Rvs161) must occur through other mechanisms yet to be defined. Based on these protein interaction data, App1p is postulated to play a role in endocytosis (67). However, until now the molecular function of App1p has been unknown. App1p PAP located at cortical actin patches (92) may regulate the local concentrations of PA and DAG. These lipids are known to facilitate membrane fission/fusion events in model systems (93–98), and they are also known to interact with and regulate enzymes (*e.g.* phosphatidylinositol 4-phosphate kinase, protein kinase C, protein kinase D) that play important roles in vesicular trafficking (99–103). For example, in mammalian cells, the inhibition of PAP activity by propranolol attenuates protein kinase D recruitment to Golgi membranes, blocking vesicle bud formation and protein transport to the cell surface (103, 104). Unfortunately, propranolol does not discriminate between Mg^{2+}-dependent and Mg^{2+}-independent PAP activities (90, 105–107), and thus, the identity of the type of PAP enzyme involved in this process is unknown. We speculate that in yeast, App1p PAP activity plays a role in vesicle formation through its recruitment from the cytosol to cortical actin patches via endocytic proteins. These proteins may tether App1p PAP to actin patches and/or serve to regulate the relative amounts of PA and DAG, which in turn contribute to the control of vesicle formation. Clearly, the work reported here provides an impetus to pursue these questions in more detail. Although an App1p homolog does not exist in higher eukaryotes, a functional homolog exists in the form of the lipin PAP enzymes that catalyze the same reaction (27, 106, 108), and as indicated above, a PAP activity is implicated in vesicular trafficking in mammalian cells.

REFERENCES

1. Smith, S. W., Weiss, S. B., and Kennedy, E. P. (1957) The enzymatic dephosphorylation of phosphatidic acids. *J. Biol. Chem.* **228,** 915–922
2. Kennedy, E. P., and Weiss, S. B. (1956) The function of cytidine coenzyme in the biosynthesis of phospholipids. *J. Biol. Chem.* **222,** 193–214
3. Borkenhagen, L. F., and Kennedy, E. P. (1957) The enzymatic synthesis of cytidine diphosphate choline. *J. Biol. Chem.* **227,** 951–962
4. Weiss, S. B., Smith, S. W., and Kennedy, E. P. (1958) The enzymatic formation of lecithin from cytidine diphosphate choline and D-1,2-diglyceride. *J. Biol. Chem.* **231,** 53– 64
5. Kennedy, E. P. (1956) The synthesis of cytidine diphosphate choline, cytidine diphosphate ethanolamine, and related compounds. *J. Biol. Chem.* **222,** 185–191
6. Weiss, S. B., Kennedy, E. P., and Kiyasu, J. Y. (1960) The enzymatic synthesis of triglycerides. *J. Biol. Chem.* **235,** 40– 44
7. Paulus, H., and Kennedy, E. P. (1960) The enzymatic synthesis of inositol monophosphatide. *J. Biol. Chem.* **235,** 1303–1311
8. Kiyasu, J. Y., Pieringer, R. A., Paulus, H., and Kennedy, E. P. (1963) The biosynthesis of phosphatidylglycerol. *J. Biol. Chem.* **238,** 2293–2298
9. Davidson, J. B., and Stanacev, N. Z. (1971) Biosynthesis of cardiolipin in mitochondria isolated from guinea pig liver. *Biochem. Biophys. Res. Commun.* **42,** 1191–1199
10. Bishop, W. R., Ganong, B. R., and Bell, R. M. (1986) Attenuation of *sn*-1,2-diacylglycerol second messengers by diacylglycerol kinase. *J. Biol. Chem.* **261,** 6993–7000
11. Kearns, B. G., McGee, T. P., Mayinger, P., Gedvilaite, A., Phillips, S. E., Kagiwada, S., and Bankaitis, V. A. (1997) Essential role for diacylglycerol in protein transport from the yeast Golgi complex. *Nature* **387,** 101–105
12. Waggoner, D. W., Xu, J., Singh, I., Jasinska, R., Zhang, Q. X., and Brindley, D. N. (1999) Structural organization of mammalian lipid phosphate phosphatases: implications for signal transduction. *Biochim. Biophys. Acta* **1439,** 299–316
13. Sciorra, V. A., and Morris, A. J. (2002) Roles for lipid phosphate phosphatases in regulation of cellular signaling. *Biochim. Biophys. Acta* **1582,** 45–51
14. Testerink, C., and Munnik, T. (2005) Phosphatidic acid: a multifunctional stress signaling lipid in plants. *Trends Plant Sci.* **10,** 368–375
15. Wang, X., Devaiah, S. P., Zhang, W., and Welti, R. (2006) Signaling functions of phosphatidic acid. *Prog. Lipid Res.* **45,** 250–278
16. Brindley, D. N. (2004) Lipid phosphate phosphatases and related proteins: signaling functions in development, cell division, and cancer. *J. Cell. Biochem.* **92,** 900–912
17. Howe, A. G., and McMaster, C. R. (2006) Regulation of phosphatidylcholine homeostasis by Sec14. *Can. J. Physiol. Pharmacol.* **84,** 29–38
18. Foster, D. A. (2007) Regulation of mTOR by phosphatidic acid? *Cancer Res.* **67,** 1–4
19. Carman, G. M., and Henry, S. A. (2007) Phosphatidic acid plays a central role in the transcriptional regulation of glycerophospholipid synthesis in *Saccharomyces cerevisiae. J. Biol. Chem.* **282,** 37293–37297
20. Carrasco, S., and Mérida, I. (2007) Diacylglycerol, when simplicity becomes complex. *Trends Biochem. Sci.* **32,** 27–36
21. Carman, G. M., and Han, G.-S. (2006) Roles of phosphatidate phosphatase enzymes in lipid metabolism. *Trends Biochem. Sci.* **31,** 694–699
22. Carman, G. M., and Han, G.-S. (2009) Phosphatidic acid phosphatase, a key enzyme in the regulation of lipid synthesis. *J. Biol. Chem.* **284,** 2593–2597
23. Csaki, L. S., and Reue, K. (2010) Lipins: multifunctional lipid metabolism proteins. *Annu. Rev. Nutr.* **30,** 257–272
24. Reue, K., and Dwyer, J. R. (2009) Lipin proteins and metabolic homeostasis. *J. Lipid Res.* **50,** (suppl.) S109–S114
25. Reue, K., and Brindley, D. N. (2008) Multiple roles for lipins/phosphatidate phosphatase enzymes in lipid metabolism. *J. Lipid Res.* **49,** 2493–2503
26. Pascual, F., and Carman, G. M. (2012) Phosphatidate phosphatase, a key regulator of lipid homeostasis. *Biochim. Biophys. Acta*, doi:10.1016/j.bbalip.2012.08.006
27. Han, G.-S., Wu, W.-I., and Carman, G. M. (2006) The *Saccharomyces cerevisiae* lipin homolog is a Mg^{2+}-dependent phosphatidate phosphatase enzyme. *J. Biol. Chem.* **281,** 9210–9218
28. Toke, D. A., Bennett, W. L., Dillon, D. A., Wu, W.-I., Chen, X., Ostrander, D. B., Oshiro, J., Cremesti, A., Voelker, D. R., Fischl, A. S., and Carman, G. M. (1998) Isolation and characterization of the *Saccharomyces cerevisiae DPP1* gene encoding for diacylglycerol pyrophosphate phosphatase. *J. Biol. Chem.* **273,** 3278–3284
29. Toke, D. A., Bennett, W. L., Oshiro, J., Wu, W.-I., Voelker, D. R., and Carman, G. M. (1998) Isolation and characterization of the *Saccharomyces cerevisiae LPP1* gene encoding a Mg^{2+}-independent phosphatidate phosphatase. *J. Biol. Chem.* **273,** 14331–14338
30. Han, G.-S., Siniossoglou, S., and Carman, G. M. (2007) The cellular functions of the yeast lipin homolog Pah1p are dependent on its phosphatidate phosphatase activity. *J. Biol. Chem.* **282,** 37026–37035
31. Stukey, J., and Carman, G. M. (1997) Identification of a novel phosphatase sequence motif. *Protein Sci.* **6,** 469–472
32. Toke, D. A., McClintick, M. L., and Carman, G. M. (1999) Mutagenesis of the phosphatase sequence motif in diacylglycerol pyrophosphate phosphatase from *Saccharomyces cerevisiae. Biochemistry* **38,** 14606–14613
33. Dillon, D. A., Chen, X., Zeimetz, G. M., Wu, W.-I., Waggoner, D. W., Dewald, J., Brindley, D. N., and Carman, G. M. (1997) Mammalian Mg^{2+}-independent phosphatidate phosphatase (PAP2) displays diacylglycerol pyrophosphate phosphatase activity. *J. Biol. Chem.* **272,** 10361–10366
34. Wu, W.-I., Liu, Y., Riedel, B., Wissing, J. B., Fischl, A. S., and Carman, G. M. (1996) Purification and characterization of diacylglycerol pyrophosphate

phosphatase from *Saccharomyces cerevisiae. J. Biol. Chem.* **271,** 1868–1876

35. Dillon, D. A., Wu, W.-I., Riedel, B., Wissing, J. B., Dowhan, W., and Carman, G. M. (1996) The *Escherichia coli pgpB* gene encodes for a diacylglycerol pyrophosphate phosphatase activity. *J. Biol. Chem.* **271,** 30548–30553

36. Faulkner, A., Chen, X., Rush, J., Horazdovsky, B., Waechter, C. J., Carman, G. M., and Sternweis, P. C. (1999) The *LPP1* and *DPP1* gene products account for most of the isoprenoid phosphatase activities in *Saccharomyces cerevisiae. J. Biol. Chem.* **274,** 14831–14837

37. Choi, H.-S., Su, W.-M., Han, G.-S., Plote, D., Xu, Z., and Carman, G. M. (2012) Pho85p-Pho80p phosphorylation of yeast Pah1p phosphatidate phosphatase regulates its activity, location, abundance, and function in lipid metabolism. *J. Biol. Chem.* **287,** 11290–11301

38. Choi, H.-S., Su, W.-M., Morgan, J. M., Han, G.-S., Xu, Z., Karanasios, E., Siniossoglou, S., and Carman, G. M. (2011) Phosphorylation of phosphatidate phosphatase regulates its membrane association and physiological functions in *Saccharomyces cerevisiae*: identification of Ser^{602}, Thr^{723}, and Ser^{744} as the sites phosphorylated by CDC28 (CDK1)-encoded cyclin-dependent kinase. *J. Biol. Chem.* **286,** 1486–1498

39. Su, W.-M., Han, G.-S., Casciano, J., and Carman, G. M. (2012) Protein kinase A-mediated phosphorylation of Pah1p phosphatidate phosphatase functions in conjunction with the Pho85p-Pho80p and Cdc28p-cyclin B kinases to regulate lipid synthesis in yeast. *J. Biol. Chem.* **287,** 33364–33376

40. Blom, N., Sicheritz-Pontén, T., Gupta, R., Gammeltoft, S., and Brunak, S. (2004) Prediction of post-translational glycosylation and phosphorylation of proteins from the amino acid sequence. *Proteomics* **4,** 1633–1649

41. Siniossoglou, S., Santos-Rosa, H., Rappsilber, J., Mann, M., and Hurt, E. (1998) A novel complex of membrane proteins required for formation of a spherical nucleus. *EMBO J.* **17,** 6449–6464

42. Karanasios, E., Han, G.-S., Xu, Z., Carman, G. M., and Siniossoglou, S. (2010) A phosphorylation-regulated amphipathic helix controls the membrane translocation and function of the yeast phosphatidate phosphatase. *Proc. Natl. Acad. Sci. U.S.A.* **107,** 17539–17544

43. Santos-Rosa, H., Leung, J., Grimsey, N., Peak-Chew, S., and Siniossoglou, S. (2005) The yeast lipin Smp2 couples phospholipid biosynthesis to nuclear membrane growth. *EMBO J.* **24,** 1931–1941

44. Han, G.-S., Johnston, C. N., Chen, X., Athenstaedt, K., Daum, G., and Carman, G. M. (2001) Regulation of the *Saccharomyces cerevisiae DPP1*-encoded diacylglycerol pyrophosphate phosphatase by zinc. *J. Biol. Chem.* **276,** 10126–10133

45. Han, G.-S., Johnston, C. N., and Carman, G. M. (2004) Vacuole membrane topography of the DPP1-encoded diacylglycerol pyrophosphate phosphatase catalytic site from *Saccharomyces cerevisiae. J. Biol. Chem.* **279,** 5338–5345

46. Huh, W. K., Falvo, J. V., Gerke, L. C., Carroll, A. S., Howson, R. W., Weissman, J. S., and O'Shea, E. K. (2003) Global analysis of protein localization in budding yeast. *Nature* **425,** 686–691

47. Fakas, S., Qiu, Y., Dixon, J. L., Han, G.-S., Ruggles, K. V., Garbarino, J., Sturley, S. L., and Carman, G. M. (2011) Phosphatidate phosphatase activity plays a key role in protection against fatty acid-induced toxicity in yeast. *J. Biol. Chem.* **286,** 29074–29085

48. Adeyo, O., Horn, P. J., Lee, S., Binns, D. D., Chandrahas, A., Chapman, K. D., and Goodman, J. M. (2011) The yeast lipin orthologue Pah1p is important for biogenesis of lipid droplets. *J. Cell Biol.* **192,** 1043–1055

49. Sasser, T., Qiu, Q. S., Karunakaran, S., Padolina, M., Reyes, A., Flood, B., Smith, S., Gonzales, C., and Fratti, R. A. (2012) The yeast lipin 1 orthologue Pah1p regulates vacuole homeostasis and membrane fusion. *J. Biol. Chem.* **287,** 2221–2236

50. Rose, M. D., Winston, F., and Heiter, P. (1990) *Methods in Yeast Genetics: A Laboratory Course Manual*, Cold Spring Harbor Laboratory Press, Cold Spring Harbor, NY

51. Sambrook, J., Fritsch, E. F., and Maniatis, T. (1989) *Molecular Cloning: A Laboratory Manual*, 2nd Ed., Cold Spring Harbor Laboratory, Cold Spring Harbor, NY

52. Ito, H., Fukuda, Y., Murata, K., and Kimura, A. (1983) Transformation of intact yeast cells treated with alkali cations. *J. Bacteriol.* **153,** 163–168

53. Innis, M. A., and Gelfand, D. H. (1990) in *PCR Protocols: A Guide to Methods and Applications* (Innis, M. A., Gelfand, D. H., Sninsky, J. J., and White, T. J., eds) pp. 3–12, Academic Press, Inc., San Diego

54. Rothstein, R. (1991) Targeting, disruption, replacement, and allele rescue: Integrative DNA transformation in yeast. *Methods Enzymol.* **194,** 281–301

55. Fischl, A. S., and Carman, G. M. (1983) Phosphatidylinositol biosynthesis in *Saccharomyces cerevisiae*: purification and properties of microsome-associated phosphatidylinositol synthase. *J. Bacteriol.* **154,** 304–311

56. Bradford, M. M. (1976) A rapid and sensitive method for the quantitation of microgram quantities of protein utilizing the principle of protein-dye binding. *Anal. Biochem.* **72,** 248–254

57. Belenduik, G., Mangnall, D., Tung, B., Westley, J., and Getz, G. S. (1978) CTP-phosphatidic acid cytidyltransferase from *Saccharomyces cerevisiae*: partial purification, characterization, and kinetic behavior. *J. Biol. Chem.* **253,** 4555–4565

58. Carman, G. M., and Lin, Y.-P. (1991) Phosphatidate phosphatase from yeast. *Methods Enzymol.* **197,** 548–553

59. Laemmli, U. K. (1970) Cleavage of structural proteins during the assembly of the head of bacteriophage T4. *Nature* **227,** 680–685

60. Burnette, W. (1981) Western blotting: Electrophoretic transfer of proteins from sodium dodecyl sulfate-polyacrylamide gels to unmodified nitrocellulose and radiographic detection with antibody and radioiodinated protein A. *Anal. Biochem.* **112,** 195–203

61. Haid, A., and Suissa, M. (1983) Immunochemical identification of membrane proteins after sodium dodecyl sulfate-polyacrylamide gel electrophoresis. *Methods Enzymol.* **96,** 192–205

62. Das, A., Li, H., Liu, T., and Bellofatto, V. (2006) Biochemical characterization of *Trypanosoma brucei* RNA polymerase II. *Mol. Biochem. Parasitol.* **150,** 201–210

63. Jain, M. R., Li, Q., Liu, T., Rinaggio, J., Ketkar, A., Tournier, V., Madura, K., Elkabes, S., and Li, H. (2012) Proteomic identification of immunoproteasome accumulation in formalin-fixed rodent spinal cords with experimental autoimmune encephalomyelitis. *J. Proteome Res.* **11,** 1791–1803

64. Bligh, E. G., and Dyer, W. J. (1959) A rapid method of total lipid extraction and purification. *Can. J. Biochem. Physiol.* **37,** 911–917

65. Esko, J. D., and Raetz, C. R. (1980) Mutants of Chinese hamster ovary cells with altered membrane phospholipid composition: replacement of phosphatidylinositol by phosphatidylglycerol in a *myo*-inositol auxotroph. *J. Biol. Chem.* **255,** 4474–4480

66. Henderson, R. J., and Tocher, D. R. (1992) in *Lipid Analysis* (Hamilton, R. J., and Hamilton, S., eds) pp. 65–111, IRL Press, New York

67. Drees, B. L., Sundin, B., Brazeau, E., Caviston, J. P., Chen, G. C., Guo, W., Kozminski, K. G., Lau, M. W., Moskow, J. J., Tong, A., Schenkman, L. R., McKenzie, A., 3rd, Brennwald, P., Longtine, M., Bi, E., Chan, C., Novick, P., Boone, C., Pringle, J. R., Davis, T. N., Fields, S., and Drubin, D. G. (2001) A protein interaction map for cell polarity development. *J. Cell Biol.* **154,** 549–571

68. Bon, E., Recordon-Navarro, P., Durrens, P., Iwase, M., Toh-E, A., and Aigle, M. (2000) A network of proteins around Rvs167p and Rvs161p, two proteins related to the yeast actin cytoskeleton. *Yeast* **16,** 1229–1241

69. Ho, Y., Gruhler, A., Heilbut, A., Bader, G. D., Moore, L., Adams, S. L., Millar, A., Taylor, P., Bennett, K., Boutilier, K., Yang, L., Wolting, C., Donaldson, I., Schandorff, S., Shewnarane, J., Vo, M., Taggart, J., Goudreault, M., Muskat, B., Alfarano, C., Dewar, D., Lin, Z., Michalickova, K., Willems, A. R., Sassi, H., Nielsen, P. A., Rasmussen, K. J., Andersen, J. R., Johansen, L. E., Hansen, L. H., Jespersen, H., Podtelejnikov, A., Nielsen, E., Crawford, J., Poulsen, V., Sørensen, B. D., Matthiesen, J., Hendrickson, R. C., Gleeson, F., Pawson, T., Moran, M. F., Durocher, D., Mann, M., Hogue, C. W., Figeys, D., and Tyers, M. (2002) Systematic identification of protein complexes in *Saccharomyces cerevisiae* by mass spectrometry. *Nature* **415,** 180–183

70. Tong, A. H., Drees, B., Nardelli, G., Bader, G. D., Brannetti, B., Castagnoli, L., Evangelista, M., Ferracuti, S., Nelson, B., Paoluzi, S., Quondam, M., Zucconi, A., Hogue, C. W., Fields, S., Boone, C., and Cesareni, G. (2002) A combined experimental and computational strategy to define protein interaction networks for peptide recognition modules. *Science* **295,** 321–324

71. Fazi, B., Cope, M. J., Douangamath, A., Ferracuti, S., Schirwitz, K., Zucconi, A., Drubin, D. G., Wilmanns, M., Cesareni, G., and Castagnoli, L. (2002) Unusual binding properties of the SH3 domain of the yeast actin-binding protein Abp1: structural and functional analysis. *J. Biol. Chem.* **277,** 5290–5298

72. Landgraf, C., Panni, S., Montecchi-Palazzi, L., Castagnoli, L., Schneider-Mergener, J., Volkmer-Engert, R., and Cesareni, G. (2004) Protein interaction networks by proteome peptide scanning. *PLoS. Biol.* **2,** E14

73. Tonikian, R., Xin, X., Toret, C. P., Gfeller, D., Landgraf, C., Panni, S., Paoluzi, S., Castagnoli, L., Currell, B., Seshagiri, S., Yu, H., Winsor, B., Vidal, M., Gerstein, M. B., Bader, G. D., Volkmer, R., Cesareni, G., Drubin, D. G., Kim, P. M., Sidhu, S. S., and Boone, C. (2009) Bayesian modeling of the yeast SH3 domain interactome predicts spatiotemporal dynamics of endocytosis proteins. *PLoS. Biol.* **7,** e1000218

74. Yu, H., Braun, P., Yildirim, M. A., Lemmens, I., Venkatesan, K., Sahalie, J., Hirozane-Kishikawa, T., Gebreab, F., Li, N., Simonis, N., Hao, T., Rual, J. F., Dricot, A., Vazquez, A., Murray, R. R., Simon, C., Tardivo, L., Tam, S., Svrzikapa, N., Fan, C., de Smet, A. S., Motyl, A., Hudson, M. E., Park, J., Xin, X., Cusick, M. E., Moore, T., Boone, C., Snyder, M., Roth, F. P., Barabási, A. L., Tavernier, J., Hill, D. E., and Vidal, M. (2008) High-quality binary protein interaction map of the yeast interactome network. *Science* **322,** 104–110

75. Michelot, A., Costanzo, M., Sarkeshik, A., Boone, C., Yates, J. R., 3rd, and Drubin, D. G. (2010) Reconstitution and protein composition analysis of endocytic actin patches. *Curr. Biol.* **20,** 1890–1899

76. Punta, M., Coggill, P. C., Eberhardt, R. Y., Mistry, J., Tate, J., Boursnell, C., Pang, N., Forslund, K., Ceric, G., Clements, J., Heger, A., Holm, L., Sonnhammer, E. L., Eddy, S. R., Bateman, A., and Finn, R. D. (2012) The Pfam protein families database. *Nucleic Acids Res.* **40,** D290-D301

77. Madera, M., Vogel, C., Kummerfeld, S. K., Chothia, C., and Gough, J. (2004) The SUPERFAMILY database in 2004: additions and improvements. *Nucleic Acids Res.* **32,** D235-D239

78. Péterfy, M., Phan, J., Xu, P., and Reue, K. (2001) Lipodystrophy in the *fld* mouse results from mutation of a new gene encoding a nuclear protein, lipin. *Nat. Genet.* **27,** 121–124

79. Feng, S., Chen, J. K., Yu, H., Simon, J. A., and Schreiber, S. L. (1994) Two binding orientations for peptides to the Src SH3 domain: development of a general model for SH3-ligand interactions. *Science* **266,** 1241–1247

80. Lim, W. A., Richards, F. M., and Fox, R. O. (1994) Structural determinants of peptide-binding orientation and of sequence specificity in SH3 domains. *Nature* **372,** 375–379

81. Hosaka, K., and Yamashita, S. (1984) Regulatory role of phosphatidate phosphatase in triacylglycerol synthesis of *Saccharomyces cerevisiae*. *Biochim. Biophys. Acta* **796,** 110–117

82. Oshiro, J., Rangaswamy, S., Chen, X., Han, G.-S., Quinn, J. E., and Carman, G. M. (2000) Regulation of the *DPP1*-encoded diacylglycerol pyrophosphate (DGPP) phosphatase by inositol and growth phase: inhibition of DGPP phosphatase activity by CDP-diacylglycerol and activation of phosphatidylserine synthase activity by DGPP. *J. Biol. Chem.* **275,** 40887–40896

83. Hanscho, M., Ruckerbauer, D. E., Chauhan, N., Hofbauer, H. F., Krahulec, S., Nidetzky, B., Kohlwein, S. D., Zanghellini, J., and Natter, K. (2012) Nutritional requirements of the BY series of *Saccharomyces cerevisiae* strains for optimum growth. *FEMS Yeast Res.* **12,** 796–808

84. Irie, K., Takase, M., Araki, H., and Oshima, Y. (1993) A gene, *SMP2*, involved in plasmid maintenance and respiration in *Saccharomyces cerevisiae* encodes a highly charged protein. *Mol. Gen. Genet.* **236,** 283–288

85. Carman, G. M., and Han, G.-S. (2011) Regulation of phospholipid synthesis in the yeast *Saccharomyces cerevisiae. Ann. Rev. Biochem.* **80,** 859–883

86. Henry, S. A., Kohlwein, S. D., and Carman, G. M. (2012) Metabolism and regulation of glycerolipids in the yeast *Saccharomyces cerevisiae. Genetics* **190,** 317–349

87. Lin, Y.-P., and Carman, G. M. (1989) Purification and characterization of phosphatidate phosphatase from *Saccharomyces cerevisiae. J. Biol. Chem.* **264,** 8641–8645

88. Hosaka, K., and Yamashita, S. (1984) Partial purification and properties of phosphatidate phosphatase in *Saccharomyces cerevisiae. Biochim. Biophys. Acta* **796,** 102–109

89. Morlock, K. R., McLaughlin, J. J., Lin, Y.-P., and Carman, G. M. (1991) Phosphatidate phosphatase from *Saccharomyces cerevisiae*: isolation of 45-kDa and 104-kDa forms of the enzyme that are differentially regulated by inositol. *J. Biol. Chem.* **266,** 3586–3593

90. Furneisen, J. M., and Carman, G. M. (2000) Enzymological properties of the *LPP1*-encoded lipid phosphatase from *Saccharomyces cerevisiae. Biochim. Biophys. Acta* **1484,** 71–82

91. Hill, J. E., Myers, A. M., Koerner, T. J., and Tzagoloff, A. (1986) Yeast/*E. coli* shuttle vectors with multiple unique restriction sites. *Yeast* **2,** 163–167

92. Weinberg, J., and Drubin, D. G. (2012) Clathrin-mediated endocytosis in budding yeast. *Trends Cell Biol.* **22,** 1–13

93. Liao, M. J., and Prestegard, J. H. (1979) Fusion of phosphatidic acid-phosphatidylcholine mixed lipid vesicles. *Biochim. Biophys. Acta* **550,** 157–173

94. Koter, M., de Kruijff, B., and van Deenen, L. L. (1978) Calcium-induced aggregation and fusion of mixed phosphatidylcholine-phosphatidic acid vesicles as studied by 31P NMR. *Biochim. Biophys. Acta* **514,** 255–263

95. Blackwood, R. A., Smolen, J. E., Transue, A., Hessler, R. J., Harsh, D. M., Brower, R. C., and French, S. (1997) Phospholipase D activity facilitates Ca^{2+}-induced aggregation and fusion of complex liposomes. *Am. J. Physiol.* **272,** C1279-C1285

96. Weigert, R., Silletta, M. G., Spanò, S., Turacchio, G., Cericola, C., Colanzi, A., Senatore, S., Mancini, R., Polishchuk, E. V., Salmona, M., Facchiano, F., Burger, K. N., Mironov, A., Luini, A., and Corda, D. (1999) CtBP/BARS induces fission of Golgi membranes by acylating lysophosphatidic acid. *Nature* **402,** 429–433

97. Goñi, F. M., and Alonso, A. (1999) Structure and functional properties of diacylglycerols in membranes. *Prog. Lipid Res.* **38,** 1–48

98. Chernomordik, L., Kozlov, M. M., and Zimmerberg, J. (1995) Lipids in biological membrane fusion. *J. Membr. Biol.* **146,** 1–14

99. Roth, M. G. (2008) Molecular mechanisms of PLD function in membrane traffic. *Traffic.* **9,** 1233–1239

100. Morris, A. J. (2007) Regulation of phospholipase D activity, membrane targeting, and intracellular trafficking by phosphoinositides. *Biochem. Soc. Symp.* 247–257

101. Maissel, A., Marom, M., Shtutman, M., Shahaf, G., and Livneh, E. (2006) PKCη is localized in the Golgi, ER, and nuclear envelope and translocates to the nuclear envelope upon PMA activation and serum-starvation: C1b domain and the pseudosubstrate containing fragment target PKCη to the Golgi and the nuclear envelope. *Cell. Signal.* **18,** 1127–1139

102. Lehel, C., Oláh, Z., Jakab, G., Szállási, Z., Petrovics, G., Harta, G., Blumberg, P. M., and Anderson, W. B. (1995) Protein kinase C ε subcellular localization domains and proteolytic degradation sites: a model for protein kinase C conformational changes. *J. Biol. Chem.* **270,** 19651–19658

103. Baron, C. L., and Malhotra, V. (2002) Role of diacylglycerol in PKD recruitment to the TGN and protein transport to the plasma membrane. *Science* **295,** 325–328

104. Asp, L., Kartberg, F., Fernandez-Rodriguez, J., Smedh, M., Elsner, M., Laporte, F., Bárcena, M., Jansen, K. A., Valentijn, J. A., Koster, A. J., Bergeron, J. J., and Nilsson, T. (2009) Early stages of Golgi vesicle and tubule formation require diacylglycerol. *Mol. Biol. Cell* **20,** 780–790

105. Jamal, Z., Martin, A., Gomez-Muñoz, A., and Brindley, D. N. (1991) Plasma membrane fractions from rat liver contain a phosphatidate phosphohydrolase distinct from that in the endoplasmic reticulum and cytosol. *J. Biol. Chem.* **266,** 2988–2996

106. Han, G.-S., and Carman, G. M. (2010) Characterization of the human *LPIN1*-encoded phosphatidate phosphatase isoforms. *J. Biol. Chem.* **285,** 14628–14638

107. Havriluk, T., Lozy, F., Siniossoglou, S., and Carman, G. M. (2008) Colorimetric determination of pure Mg^{2+}-dependent phosphatidate phosphatase activity. *Anal. Biochem.* **373,** 392–394

108. Donkor, J., Sariahmetoglu, M., Dewald, J., Brindley, D. N., and Reue, K. (2007) Three mammalian lipins act as phosphatidate phosphatases with distinct tissue expression patterns. *J. Biol. Chem.* **282,** 3450–3457

109. Brachmann, C. B., Davies, A., Cost, G. J., Caputo, E., Li, J., Hieter, P., and Boeke, J. D. (1998) Designer deletion strains derived from *Saccharomyces cerevisiae* S288C: a useful set of strains and plasmids for PCR-mediated gene disruption and other applications. *Yeast* **14,** 115–132

110. Thomas, B. J., and Rothstein, R. (1989) Elevated recombination rates in transcriptionally active DNA. *Cell* **56,** 619–630